Supplement: Band gaps and phonons of quasi-bulk rocksalt ScN

Jona Grümbel,* Rüdiger Goldhahn, and Martin Feneberg
Institut für Physik, Otto-von-Guericke-Universität Magdeburg, Universitätsplatz 2, 39106, Magdeburg, Germany

Yuichi Oshima
Research Center for Electronic and Optical Materials, National Institute for Materials Science , 1-1 Namiki, Tsukuba, Ibaraki 305-0044, Japan

Adam Dubroka
Department of Condensed Matter Physics, Masaryk University, Kotlářská 2, 611-37 Brno, Czech Republic

Manfred Ramsteiner
Paul-Drude-Institut für Festkörperelektronik (PDI), Hausvogteiplatz 5-7, 10117, Berlin, Germany

SI. EXPERIMENTAL SETUPS

For our ellipsometry/reflectivity measurements we use three different machines, where the WVASE32 ellipsometry software (Woollam) was used for both data recording and analyzing:

(I) A Wollam VASE rotating compensator UV ellipsometer for 0.5−6.5 eV with a HS190 monochromator and a high pressure Xe-lamp as light source. The spectral resolution trace is shown in Fig. S3.

(II) A Woollam VASE fourier transform IR ellipsometer for 280−6000 cm^{-1} (35−750 meV) with a Carbon Globar driven Michelson-Morley Interferometer as light source. The spectral resolution (energy step width) is set to 2 cm^{-1}.

(III) A Bruker Vertex 70V spectrometer for 60−700 cm^{-1}, equipped with a Hg lamp as source and DTGS detector. The spectral resolution is set to 1 cm^{-1}.

Raman measurements are recorded with two different machines:

(I) A Tri-Vista Raman microscope with an incident laser wavelength of 532.1 nm, an Olympus BX50 microscope with a x50 objective for focussing, a Princeton Instruments SP2750i monochromator with a focal length of 750 mm, grating parameter of 1800 mm^{-1}, slit width of 200 µm and a peltier-cooled charge coupled device (CCD) camera (2048px horizontal).

(II) A Horiba LabRam HR evolution system with incident laser wavelength of either 632.8 nm, or 472.9 nm, a x50 objective for focussing, a focal length of 800 mm, grating parameters of 1800 mm^{-1} or 600 mm^{-1}, slit width of 200 µm and a lN_2-cooled Symphony CCD camera (1024px horizontal).

Different setups used to record Raman/PL spectra result in the following spectral resolutions Δk_{rel} at 300 cm^{-1} ($\Delta\lambda \approx$ slit width/(grating × focal length)):

Setup 1: 633 nm, grating 1800 mm^{-1}: $\Delta k_{\mathrm{rel}} = 3.3\,\mathrm{cm}^{-1}$

Setup 2: 532 nm, grating 1800 mm^{-1}: $\Delta k_{\mathrm{rel}} = 4.8\,\mathrm{cm}^{-1}$

Setup 3: 473 nm, grating 1800 mm^{-1}: $\Delta k_{\mathrm{rel}} = 6.0\,\mathrm{cm}^{-1}$

Setup 4: 473 nm, grating 600 mm^{-1}: $\Delta k_{\mathrm{rel}} = 18\,\mathrm{cm}^{-1}$ (2 meV)

Setups 1-3 are used only for Raman measurements (Fig. 4a of the main article) and Setup 4 for the combined Raman/PL measurement (Fig. 4b of the main article).

* jona.gruembel@ovgu.de

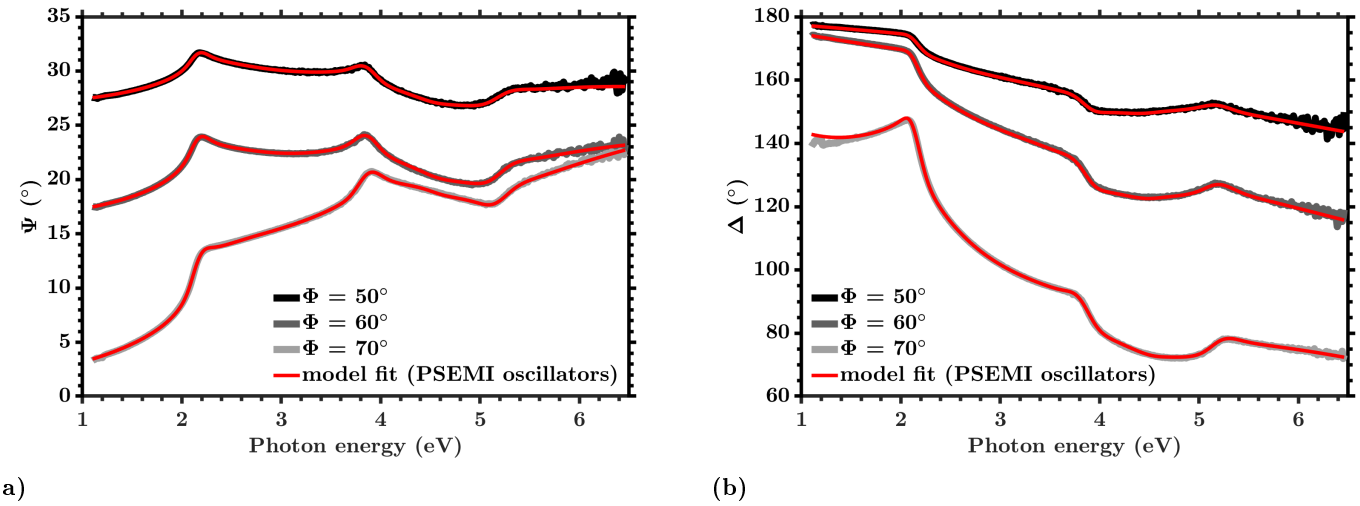

Figure S1: Parametric semiconductor (PSEMI) oscillator model fits applied to (a) Ψ and (b) Δ of UVSE before point-by-point fitting.

SII. ELLIPSOMETRY PROCEDURE

In the NIR/VIS/UV spectral range we model two layers: (I) a surface roughness layer, which we model by using a Bruggemann effective-medium layer with a void/layer ratio of 50% and a variable layer thickness and (II) the ScN film layer, which is constructed by various oscillators as shown in Fig. 3b in the main article. Due to the large thickness of our ScN films we treat them as bulk material and therefore apply no substrate model. In Figs. S1a and S1b it is obvious, that already the applied model matches the experimental data nearly perfectly and hence, since the WVASE model functions are inherently Kramers-Kronig-consistent, the NIR-UV dielectric function determined from point-by-point fitting is Kramers-Kronig-consistent. In the IR/FIR spectral range only a single layer for the ScN film is used. The bulk approach is further supported by the absence of Fabry-Perot-oscillations in the NIR/VIS range and the absence of sapphire substrate contributions in the MIR range (see Figs. 2a and 2b in the main article).

SIII. RAMAN SPECTRA LINE SHAPE FITS

For quantitative analysis we determine the energy positions by line shape fits. There, we deal with two problems: (I) the underlying luminescence signal and (II) the non-Lorentzian line shape of some signals. The non-Lorentzian line shape can either arise from coupling with free charge carriers or from even number TO phonons. As discussed in the main article, previous XRD results suggest that those signal possibly stem from the even number TO lines because they exhibit $2\omega_{\mathrm{TO}} \approx \omega_{\mathrm{LO}}$. The first order Raman scattering intensity typically exhibits Lorentzian type line shapes, given by

$$I(\omega) = \frac{A\gamma^2}{4(\omega-\omega_0)^2+\gamma^2} \tag{1}$$

with amplitude A, eigenfrequency ω_0, and broadening γ. We apply a local linear background, fitting each peak individually for best fit results. In total, we have

$$I(\omega) = I_0 + m\omega + \frac{A\gamma^2}{4(\omega-\omega_0)^2+\gamma^2} \tag{2}$$

where m is an arbitrary but linear slope and I_0 a constant background.

In Figs. S2a-S2h fit results of all evaluated phonon lines are shown. The applied model matches well with the data, only for the 2LO signal small deviations are visible.

SIV. ERRORS

For values directly extracted as fit parameters the given errors in Tabs. 1 and 2 of the main article display the 99.5% confidence bounds of the fit. For the derived parameters ε_∞, $\varepsilon_{\mathrm{stat}}$, Z^*, $\omega_{\mathrm{LO}}^{(\mathrm{LST})}$ and the LST-relation probe, the errors are

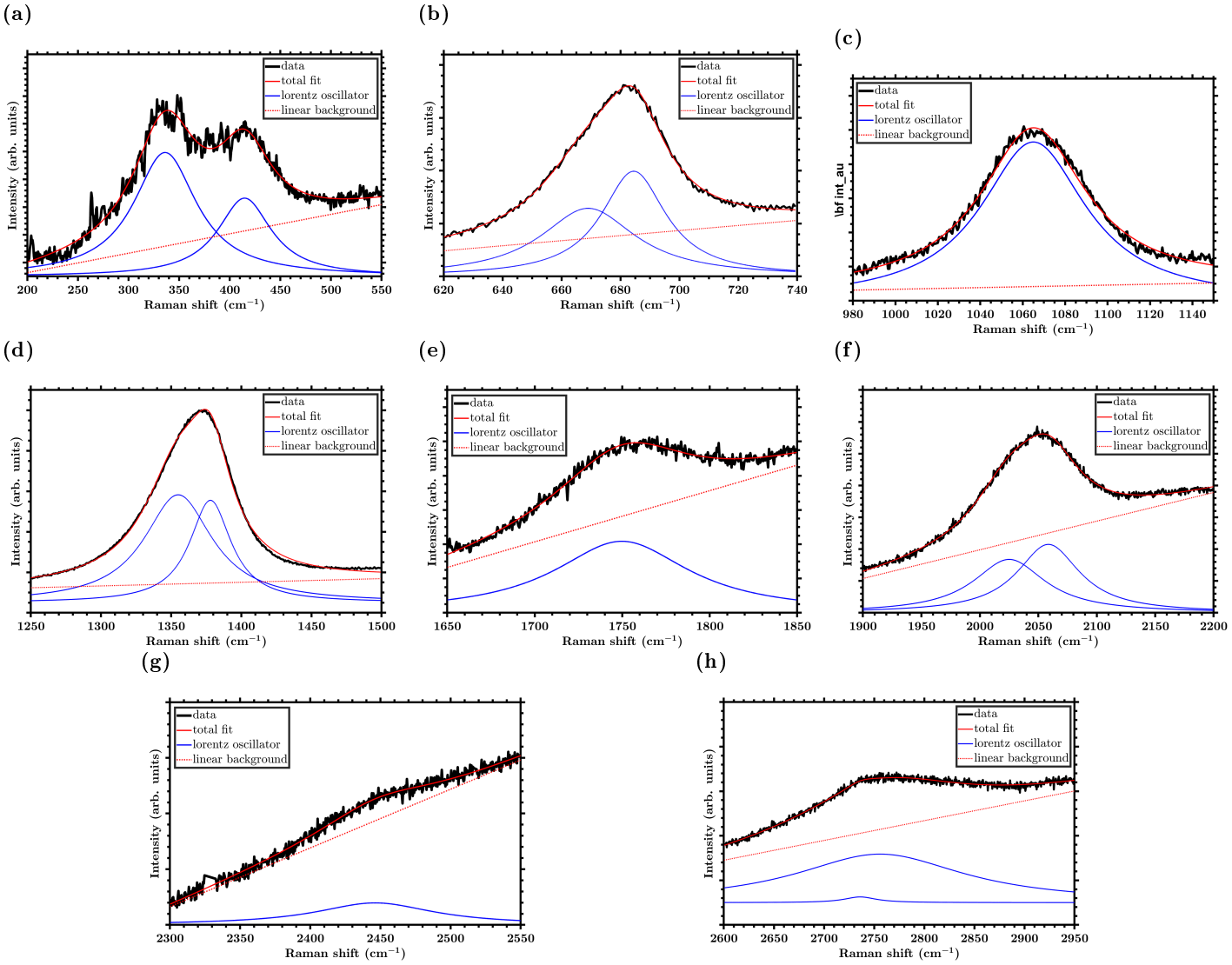

Figure S2: Fit results at nLO/TO-spectral regions of the Raman spectrum with $E_{\mathrm{Laser}} = 2.62\,\mathrm{eV}$.

calculated using linear error propagation law and the corresponding fit errors of the required parameters. For the transition energies E_Γ and $E_{\Gamma'}$, which display via splinefit determined inflection points of ε_2, the error is set as the spectral resolution of the UV ellipsometer at the corresponding photon energy (see Fig. S3). For the indirect bandgap the error is an estimate for our scale-reading precision when deriving it from $\langle\varepsilon_1\rangle$.

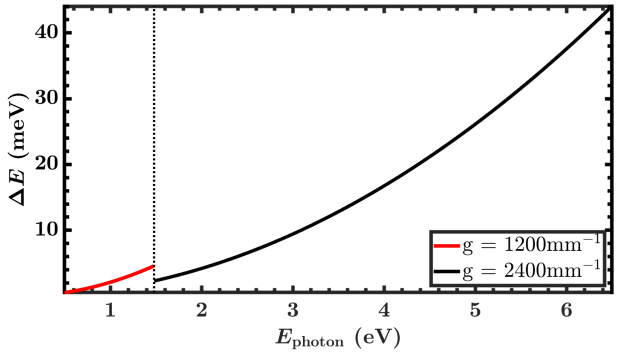

Figure S3: Spectral resolution trace of the UVSE machine. Note, that we use auto slit mode but calculated the error with a constant $d_{\mathrm{slit}} = 500\,\mu\mathrm{m}$, which is the maximum allowed slit width.